

Image Fusion Using an Integrated, Dual-Head Coincidence Camera with X-Ray Tube–Based Attenuation Maps

James A. Patton, Dominique Delbeke, and Martin P. Sandler

Department of Radiology and Radiological Sciences, Vanderbilt University Medical Center, Nashville, Tennessee

The purpose of this study was to characterize a dual-head gamma camera capable of FDG imaging using coincidence detection and equipped with an integrated x-ray transmission system for attenuation correction, anatomic mapping, and image fusion. **Methods:** Radiation dose (425 mrad skin dose) and tissue contrast (0.7% deviation from expected values) were assessed for the x-ray system. Registration of transmission and emission scans was validated using a hot sphere phantom and was verified in selected patient studies. **Results:** Fusion of anatomic maps and FDG images allowed precise anatomic localization of lesions identified using dual-head coincidence imaging. **Conclusion:** The combined approach of x-ray attenuation, anatomic mapping, and image fusion with scintigraphic studies provides a new diagnostic tool for nuclear medicine and fertile ground for future research.

Key Words: x-ray attenuation; coincidence imaging; image fusion

J Nucl Med 2000; 41:1364–1368

Multiple indications for functional imaging using FDG now are well accepted in the fields of neurology, cardiology, and oncology (1). The clinical utility of FDG imaging first was established using dedicated PET tomographs equipped with multiple rings of bismuth germanate detectors. More recently, gamma camera–based positron imaging has become available—first using SPECT with high-energy collimators, and then using dual-head coincidence (DHC) detection with multihead gamma cameras; the latter has the advantage of significantly improved spatial resolution over the SPECT technique (2). The sensitivity of these systems has been improved by increasing NaI(Tl) crystal thickness (2), and the quality of the images has been improved further through the use of iterative reconstruction algorithms instead of filtered backprojection. These developments have increased the demand for FDG, and commercial companies have responded with improvements in the distribution of

FDG that have made the radiopharmaceutical more readily available to many medical centers.

It has been demonstrated that attenuation effects are much more significant in coincidence imaging than in SPECT because both photons from an annihilation process must pass through the region without interaction. Attenuation effects in coincidence imaging produce regional nonuniformities, distortions of intense structures, and edge effects. The implementation of attenuation correction alleviates these artifacts. Correction for attenuation effects can be performed using calculated geometric attenuation for uniform structures that are predictable in shape and content, such as the brain. For the body, various methods have been developed to provide anatomic maps of tissue distributions based on measured attenuation using radioactive transmission sources. Each pixel in an anatomic map is the linear attenuation coefficient of the tissues represented by that pixel. The quality of the final emission image that is corrected for attenuation effects using these anatomic maps largely depends on registration of the transmission and emission scans, which often depends on accurate repositioning of the patient in the scanner gantry between transmission and emission imaging, and motion of the patient during long scanning times.

Interpretation of emission scans in oncological applications often is complicated by the absence of detailed anatomy in the emission images. In practice, interpretation is accomplished by visually comparing the emission scans with high-quality anatomic maps provided by clinical CT scanners. The emission scan also can be registered with the anatomic maps using mathematical algorithms and anatomic markers that appear in both sets of images or by using more sophisticated methods involving calculus-based techniques (3). These images can be overlaid (fused) to provide anatomic location of the detected abnormalities. These methods often suffer from registration errors, however, due to difficulties in patient repositioning and movement of internal organs between scanning sessions. Recently, a commercial CT scanner and a commercial, dedicated PET scanner have been integrated and mounted on a single support system with a common imaging table (4). The

Received Jun. 28, 1999; revision accepted Oct. 3, 1999.

For correspondence or reprints contact: James A. Patton, PhD, Department of Radiology and Radiological Sciences, Vanderbilt University Medical Center, 21st Ave. S. and Garland, Nashville, TN 37232–2675.

combined system provides high-quality anatomic maps that can be used for attenuation correction of PET emission scans acquired (and registered) with the same system. Image fusion also can be performed for anatomic correlation. A combined CT and SPECT system using a common detector also is being developed to provide anatomic maps for attenuation correction and fusion of SPECT emission scans (5). However, this system currently does not have coincidence imaging capability. In this study, we describe a dual-head gamma camera capable of FDG imaging using coincidence detection and equipped with an integrated x-ray transmission system to provide anatomic maps for attenuation correction and fusion with the emission scans. The purposes of this study were to characterize the system with phantom experiments, to evaluate the quality of the FDG and CT images in patients referred for evaluation of malignancies, and to demonstrate the usefulness of the fusion images for anatomic mapping.

MATERIALS AND METHODS

Physical Measurements

An x-ray tube and linear detector array were installed on a dual-head scintillation camera, with coincidence imaging capability, to provide attenuation maps and anatomic localization (Fig. 1). The scintillation camera (Millennium VG; General Electric Medical Systems, Milwaukee, WI) was equipped with 5/8-in. (15.9-mm) thick NaI(Tl) crystals and a slip-ring gantry permitting data acquisition while the detectors were continually rotating around the patient. The x-ray tube and linear detector array are mounted on the slip-ring gantry and rotate together in a fixed geometry for data acquisition. The x-ray tube operates in the continuous output mode during acquisition of each transverse slice, and the output is selectable up to a maximum of 140 kVp at 2.5 mA. The detector array consists of 384 solid state detectors (each 1.8×28 mm). The x-ray tube is collimated to provide a fanbeam of photons expanding to fill the field of view of the linear array in the transverse direction (see insert in Fig. 1) and a beam width of 1 cm at the center of the scan field in the axial direction. Because the fanbeam is wide

enough to cover the full width of the patient and because the x-ray tube and detector array are in a fixed geometry and rotate together, this system has the characteristics of a third-generation CT scanner.

For data acquisition, the patient is first positioned for x-ray transmission scanning, and 40 transverse slices are imaged as the patient is indexed through the imaging field of the transmission device using the computer-controlled imaging table. For transmission scanning, the system rotates at 2.6 revolutions per minute, with a single slice being imaged in 13.8 s and requiring 0.6 rotations (0.5 rotations plus the width of the fanbeam). Forty slices are acquired in 9.2 min. At the completion of transmission scanning, the patient is automatically repositioned so that the 40-cm axial field that was just scanned matches the 40-cm axial field of view of the dual-head scintillation camera. A 30-min coincidence scan is acquired in list mode with the detectors rotating at 1 revolution per 3 min.

Although the spatial resolution of the transmission scans is on the order of 1 mm, the scans are reconstructed into a 128×128 array (pixel size of 4.2 mm) of attenuation maps using filtered backprojection to correspond to the array size of the reconstructed emission scan. The attenuation maps are displayed using Hounsfield units to correspond to the displays routinely used in x-ray CT. The emission scan is reconstructed using an iterative reconstruction algorithm based on the ordered subsets expectation maximization (OSEM) algorithm, but modified to handle list mode data as input and using a ray-tracing algorithm for image reconstruction. This algorithm, coincidence OSEM (COSEM), uses subsets of data ordered in time (a single 180° coincidence acquisition provides a complete set of image data) instead of space, as with the conventional OSEM algorithm. During the iterative reconstruction process, each ray of emission data is corrected for attenuation using the previously acquired attenuation maps that have been scaled to 511 keV for this purpose. Sensitivity profile corrections also are performed during image reconstruction. The attenuation maps and emission images also are automatically reformatted into sagittal and coronal views from the transverse sections.

The emission images are displayed with the corresponding registered attenuation maps. Because the emission images and the transmission scans were registered precisely during acquisition, acquired using the same acquisition system, and reconstructed into

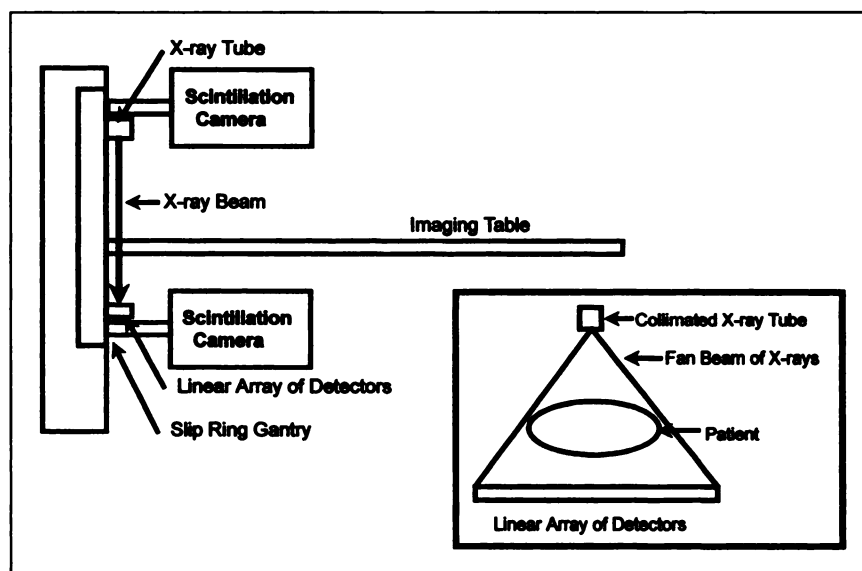


FIGURE 1. Schematic of dual-head scintillation camera with collimated x-ray tube and linear array of detectors mounted on slip-ring gantry of camera for transmission scanning. Note that transmission device is actually positioned at 90° E with respect to position of scintillation camera detectors.

the same array dimensions and identical pixel sizes, the emission images can be superimposed (fused) with the attenuation maps to provide accurate anatomic locations of detected abnormalities.

Radiation dose measurements for the x-ray system were performed using a 16-cm-diameter tissue-equivalent phantom and a pencil ionization chamber. The radiation dose from scattered radiation also was measured at 1 meter axially from the phantom using a handheld ionization chamber. The accuracy of tissue attenuation measurements was evaluated using a tissue-equivalent phantom with sections of air, water, and soft-tissue-equivalent material.

The accuracy of registration between the transmission scans and the emission images was evaluated by scanning a 22-cm diameter phantom filled with a solution of ^{18}F and containing 6 spherical inserts ranging in size from 1.3–3.8 cm in diameter and containing a solution of ^{18}F with an activity 5 times that of the volume background. Transmission and emission scans were performed, and an image of a transverse slice through the spheres was obtained and fused for evaluation purposes.

Patient Population

Twelve patients referred for an FDG PET scan (ECAT 933; Siemens, Iselin, NJ) were included in the study. All patients presented with suspected or known malignancies: 11 in the body and 1 in the brain. These patients ranged between 36 and 73 y of age (mean \pm SD = 52.7 \pm 14). There were 10 men and 2 women. All patients fasted for 4 h before imaging and had both PET and DHC imaging after the same administration of FDG. The institutional review board approved the protocol, and all patients gave their written informed consent.

FDG Imaging with the Dual-Head Gamma Camera Using Positron Coincidence Detection

DHC images were acquired after the intravenous administration of 370 MBq (10 mCi) and after PET acquisition. The time between the injection of FDG and DHC imaging was approximately 120 min. The acquisition time was 30 min over the region of interest that was selected, according to the findings on the diagnostic CT or PET images. The images were reconstructed using the COSEM algorithm. Attenuation correction was performed using attenuation maps generated from the CT transmission images.

RESULTS

Physical Measurements

The radiation dose for the x-ray system, measured at the center of a 16-cm-diameter tissue-equivalent phantom, was 336 mrad/slice and at the surface (skin dose) 425 mrad/slice. The radiation dose from scattered radiation measured at 1 m axially from the phantom was 1.0 mrad/slice (40 slices).

The errors in expected tissue attenuation coefficients acquired from a tissue contrast phantom using the x-ray system were 0.7% (air), 0.6% (water), and 0.7% (soft tissue) compared with the means of values obtained from 5 state-of-the-art CT scanners using the same phantom. Visual inspection of the fused image of a transmission scan and emission image of a hot sphere phantom could not demonstrate any misregistration within the image.

Patient Studies

The indications for FDG imaging in the 12 patients were indeterminate pulmonary nodule ($n = 1$), suspected metastatic lung carcinoma ($n = 3$), staging recurrent melanoma ($n = 2$), staging recurrent colorectal carcinoma ($n = 2$), staging gastric carcinoma ($n = 1$), monitoring therapy of lymphoma ($n = 1$), monitoring therapy of bladder carcinoma ($n = 1$), and differentiated radiation necrosis from recurrent glioblastoma multiforme ($n = 1$). Ten of the 12 patients were found to have 15 foci of FDG uptake on DHC images suggesting malignant lesions. Three patients had multiple foci of uptake at the same site that were counted as a cluster. On CT, these lesions ranged in size between 0.8 and 4 cm. In all patients, the fusion CT/DHC images helped to precisely localize the lesion on the diagnostic CT scan. Figure 2 shows images of 2 patients for whom anatomic mapping of the lesions was particularly helpful.

The first patient had known colorectal carcinoma metastatic to the liver and was evaluated for regional therapy to the liver with an infusion pump in the hepatic artery (Fig. 2A, B, C). The fused CT/FDG images demonstrated that 1 focus of uptake was located in a vertebral body. This finding changed the management to systemic chemotherapy and spared this patient a laparotomy for placement of a hepatic artery infusion pump.

The second patient (Fig. 2D, E, F) had a left pneumectomy for nonsmall cell carcinoma and presented with a new nodule in the right lung. The fusion images helped to precisely localize a second focus of uptake in the mediastinum to a lymph node that did not meet the size criteria by CT to be malignant.

In this limited study of 12 patients, added clinical value was provided by the fusion of the emission scans and anatomic maps in 3 patient studies. By providing precise anatomic localization of regions of increased metabolism, the availability of this technology caused a review of the diagnostic CT scans to be performed and a re-evaluation of the therapy plan in these patients.

DISCUSSION

The use of an x-ray tube-based transmission scan provides attenuation-corrected emission images of high quality because of the high photon flux inherent with this technique. Using the x-ray transmission scan for attenuation correction adds value because of the elimination of attenuation artifacts and improvement in image contrast. An added benefit of the availability of the x-ray transmission scan is the provision of an anatomic map for correlation/fusion with the emission scans. Although numerous investigators have demonstrated that PET imaging provides increased sensitivity/specificity versus CT in differentiating benign from malignant lesions, staging primary cancer with metastatic disease, and monitoring therapeutic response of radiation and chemotherapy, the inability of PET to provide anatomic localization remains a significant impairment in maximizing its clinical utility.

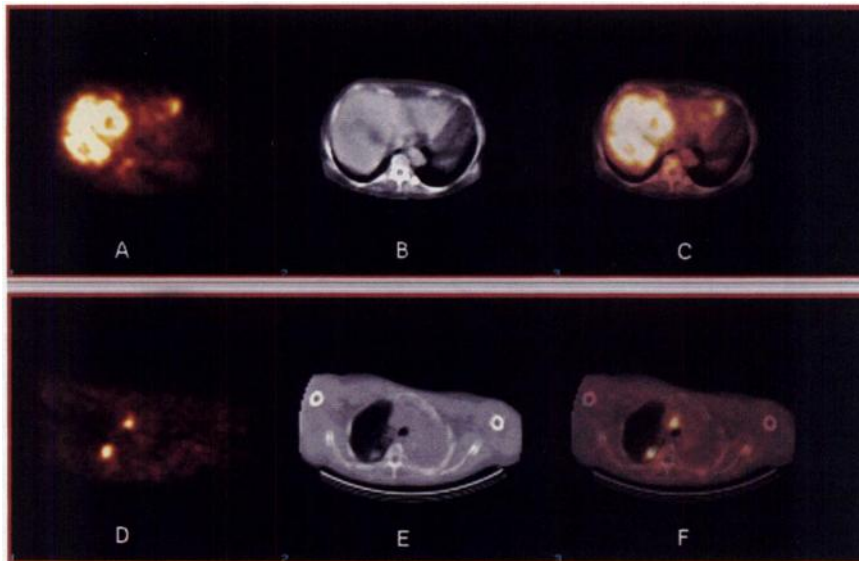


FIGURE 2. (A–C) 73-y-old woman who had sigmoid colectomy 4 mo before for colon carcinoma and was found to have multiple liver metastases. (A) The FDG image shows multiple foci of uptake in liver and 1 focus of uptake more medially that can possibly be located in spine. (B) Corresponding CT image shows multiple low-density lesions in liver. The bone window image on diagnostic CT showed no evidence of vertebral metastasis. (C) Fusion of FDG and CT images confirms localization of medial focus of uptake in vertebral body. MRI of spine confirmed vertebral metastasis. (D–F) 62-y-old man who had left pneumectomy for nonsmall cell lung carcinoma. He presents with new right lung nodule. (D) FDG image shows marked FDG uptake in right lung nodule; in addition, FDG uptake is seen in mediastinum, indicating a mediastinal lymph node involved with tumor. (E) Corresponding CT images show pleural-based nodule posteriorly in right upper lobe. (F) Fusion of FDG and CT images demonstrates superimposition of 1 focus of uptake to lung nodule. The other focus of uptake projects between trachea and aorta, where 8-mm lymph node was seen on dedicated CT scan, indicating that this small lymph node is involved by tumor.

Acceptable co-registration can be obtained using methods such as surface fitting techniques for the brain, but applications of these methods are much more difficult for body imaging. Precise anatomic localization and image fusion is greatly enhanced when using an integrated system because the patient is imaged in precisely the same position and body habitus for both the anatomic maps and PET imaging. The integration of a diagnostic CT scanner and a dedicated PET scanner provides this capability. Because a majority of patients referred for PET scanning have already had a previous diagnostic CT scan before referral, however, the need to use diagnostic quality CT for anatomic localization provides limited added value and increased expense.

The combination of the x-ray tube-based transmission device and a dual-head scintillation camera with coincidence imaging capability provides an integrated system with the expanded capabilities of attenuation correction and image fusion. Although coincidence imaging with the scintillation camera is currently inferior to that obtained with dedicated PET scanners in some instances, this new system appears to have a place in diagnostic nuclear medicine with specific applications in lesion localization and post-therapy follow-up. A final advantage of the integrated system described in this study is its ability to perform x-ray attenuation correction and image fusion for SPECT procedures and image fusion for planar imaging with single-photon emitters in common use.

CONCLUSION

This technology does not challenge the need for a high-quality diagnostic CT scan with oral and intravenous contrast administration, which is necessary to evaluate the extent of the lesions and relationship to vascular structures. However, fusion of anatomic maps and FDG images obtained sequentially in time and registered in an integrated system without patient movement allows precise anatomic localization of lesions that have increased metabolism. Anatomic localization and fusion imaging using a combined x-ray and dual-head coincidence camera may provide adequate information to accurately localize lesions with increased metabolism. In those patients where there is insufficient information to localize a lesion, the data may be used to more precisely define the appropriate slice for review from a diagnostic quality CT scan that matches up with the area of increased metabolism.

The combined approach of x-ray attenuation correction and image fusion with scintigraphic imaging provides fertile ground for future developmental research. It is a new and potentially powerful diagnostic tool for nuclear medicine imaging, radiation therapy, and surgical planning.

ACKNOWLEDGMENTS

The authors thank Barbara Sammons for preparing the manuscript and Gerry Harden and John Bobbitt for prepar-

ing the illustrations. The authors also thank Adi Balan and Albert Lon for their expert technical help in acquiring the images. This work was supported by a research grant from ELGEMS, Ltd. (Haifa, Israel) and from General Electric Medical Systems (Milwaukee, WI).

REFERENCES

1. Delbeke D. Oncological applications of FDG PET imaging: brain tumors, colorectal cancer, lymphoma, and melanoma. *J Nucl Med.* 1999;40:591-603.
2. Boren EB, Delbeke D, Patton JA, Sandler MP. Comparison of FDG PET and positron coincidence detection imaging using a dual-head camera with 5/8-inch NaI(Tl) crystals in patients with suspected body malignancies. *Eur J Nucl Med.* 1999;26:379-387.
3. Woods RP, Grafton ST, Holmes CJ, et al. Automated image registration: I. General methods and intrasubject, intramodality validation. *J Comput Assist Tomogr.* 1998;22:139-152.
4. Townsend DW, Beyer T, Kinahan PE, et al. Fusion imaging for whole-body oncology with a combined PET and CT scanner [abstract]. *J Nucl Med.* 1999;40(suppl):148P.
5. Hasegawa BH, Gingold EL, Reilly SM, et al. Description of a simultaneous emission-transmission CT system. *Proc Soc Phys in Engineering.* 1990;1231:50-60.